Supplement of Atmos. Chem. Phys., 20, 13735–13751, 2020
https://doi.org/10.5194/acp-20-13735-2020-supplement

Atmospheric Chemistry and Physics
Open Access

Supplement of

The evolution of cloud and aerosol microphysics at the summit of Mt. Tai, China

Jiarong Li et al.

Correspondence to: Jianmin Chen (jmchen@fudan.edu.cn) and Hui Chen (hui_chen@fudan.edu.cn)

Supplement Information

The influences of topography and updraft velocity on microphysical parameters during CP-1 and CP-2

The topography of the monitoring position could provide an estimate of the vertical wind field (updraft velocity, v_{up}) (Verheggen et al., 2007). Based on assumptions of air flow lines paralleling to the terrain without occurrence of sideways convergence and divergence, v_{up} was estimated by the topography of Mt. Tai and the horizontal wind speed (v_h) measured at the observation station (Hammer et al., 2014), the calculation equation was:

$$v_{up} = \tan(\alpha) \times v_h$$

Where α represented the inclination angle, which was estimated from the altitudes of Tai'an City and the summit of Mt. Tai and the horizontal distance between them (Fig. S3). It should be noticed that the calculated v_{up} could be considered as the upper limit of the true updraft velocity if the flow lines would not strictly follow the terrain (Hammer et al., 2014). As shown in Table S2 and Fig. S4, the mean $\pm$ standard deviation values of v_{up} during two focused cloud processes (CP-1 and CP-2) studied in this study was 0.82 $\pm$ 0.29 m s^{-1} and 0.92 $\pm$ 0.36 m s^{-1}, respectively. Thus, we simply assumed that the influence of v_{up} on cloud microphysical properties during CP-1 and CP-2 was relatively same.

In order to estimate the sampling losses due to wind speed and wind direction, the sampling efficiency (contributed by aspiration efficiency and transmission efficiency) was estimated based on the study of Spiegel et al. (2012). The sampling efficiency was depended on two parameters. One is sampling angle (θ_s) which is equal to α. The other is R_V which is equal to the ratio of surrounding wind speed (U_0) with sampling speed (U) of FM-120:

$$R_V = \frac{U_0}{U} = \frac{\frac{v_h}{\cos(\alpha)}}{U}$$

As shown in Fig. S3, θ_s of CP-1 and CP-2 were 11.9 ° and 10.6 °, respectively. Then, R_V of CP-1 and CP-2 were calculated based on the equation above and resulted in 0.8 and 1.0, respectively. According to the calculation provided by Spiegel et al. (2012), the aspiration efficiency and transmission efficiency of FM-120 during CP-1 and CP-2 were all close to 1. Thus, we assumed that the influences of topography and updraft velocity on Fog Monitor were small and could be ignored during CP-1 and CP-2.

Table S1. Monitoring times of cloud events with the average $PM_{2.5}$ mass concentration, cloud droplet number concentration (N_C), mean liquid water content (LWC), effective radius (r_{eff}), geometrical mean diameter (GMD), droplet surface area (PSA), pressure (P), temperature (T), relative humidity (RH), wind direction (WD), wind speed (WS) and the number of cloud samples at Mt. Tai.

Event	Start	Stop	Duration	$PM_{2.5}$	N_C	LWC	r_{eff}	$GMDc$	PSA	P	T	RH	WD	WS	No.of Sample
	(UTC/GMT 8)	(UTC/GMT 8)	(h)	(μg m^{-3})	(cm^{-3})	(g m^{-3})	(μm)	(μm)	(cm^2 m^{-3})	(hPa)	(℃)	(%)	(°)	(m s^{-1})	
1	2018/06/17 08:49	2018/06/17 09:08	0.3	34.48	156	0.03	3.9	6.8	234	84.4	14.9	90.8	203.6	1.3	0
2	2018/06/18 01:24	2018/06/18 03:02	1.6	23.23	202	0.02	3.3	5.7	268	84.2	13.3	98.8	241.1	4.1	0
3	2018/06/18 23:17	2018/06/19 00:05	0.8	44.18	300	0.06	4.1	6.4	469	84.0	14.7	97.3	233.3	3.1	0
4	2018/06/19 22:32	2018/06/19 23:26	0.9	87.65	385	0.05	3.7	5.6	478	84.3	16.0	97.8	95.0	1.9	0
5	2018/06/24 23:37	2018/06/25 22:14	22.6	7.92	558	0.35	6.8	9.4	1550	84.2	18.2	99.8	197.1	6.4	2
6	2018/06/27 23:31	2018/06/28 00:52	1.3	27.61	316	0.09	4.8	6.6	635	84.0	19.3	97.6	267.1	5.2	0
7	2018/07/01 22:40	2018/07/02 00:40	2.0	6.10	620	0.59	7.1	10.0	2481	84.2	16.6	99.2	93.4	4.2	1
8	2018/07/02 05:26	2018/07/02 08:15	2.8	31.00	402	0.06	3.6	5.9	484	84.2	16.2	98.9	58.8	3.3	0
9	2018/07/02 21:06	2018/07/02 22:02	0.9	66.02	240	0.02	3.0	4.9	230	84.1	16.4	98.5	90.7	3.0	0
10	2018/07/03 02:58	2018/07/03 06:31	3.6	41.65	380	0.07	4.0	5.9	719	83.9	15.8	97.6	34.2	4.6	0
11	2018/07/05 00:15	2018/07/05 06:25	6.2	46.44	730	0.11	3.8	5.6	1082	83.9	16.8	99.1	86.3	7.2	0
12	2018/07/05 21:35	2018/07/06 08:42	11.1	40.06	677	0.10	3.8	5.5	1137	84.2	17.4	98.8	73.2	8.6	1
13	2018/07/07 00:38	2018/07/07 02:00	1.4	28.18	462	0.06	3.6	5.4	606	84.4	16.1	98.7	98.6	4.8	0
14	2018/07/07 22:35	2018/07/08 03:00	4.4	14.68	193	0.06	5.1	6.8	456	84.4	15.9	99.8	203.6	4.8	1
15	2018/07/08 11:32	2018/07/08 22:30	11.0	20.01	440	0.14	4.9	7.2	963	84.5	16.0	97.4	89.9	5.7	2
16	2018/07/09 05:39	2018/07/09 12:18	6.6	2.99	59	0.14	9.8	12.4	525	84.5	16.0	99.6	72.6	5.8	0
17	2018/07/09 15:42	2018/07/09 22:14	6.5	11.14	166	0.07	5.3	6.6	625	84.5	15.8	93.5	92.9	2.4	0
18	2018/07/10 02:10	2018/07/10 04:55	2.7	8.17	121	0.10	6.9	8.1	627	84.5	15.5	95.6	207.1	3.4	0
19	2018/07/10 10:54	2018/07/13 12:51	74.0	8.71	633	0.32	6.0	8.4	1669	84.5	18.5	99.4	180.7	4.4	12
20	2018/07/13 21:17	2018/07/14 10:35	13.3	6.20	1519	0.54	5.2	7.5	3133	84.3	19.7	100.0	147.6	5.6	1

Continue

Event	Start (UTC/GMT 8)	Stop (UTC/GMT 8)	Duration (h)	$PM_{2.5}$ (μg m^{-3})	N_C (cm^{-3})	*LWC* (g m^{-3})	r_{eff} (μm)	*GMDc* (μm)	*PSA* (cm^2 m^{-3})	*P* (hPa)	*T* (℃)	*RH* (%)	*WD* (°)	*WS* (m s^{-1})	No.of Sample
21	2018/07/14 15:58	2018/07/15 14:09	22.2	5.80	1081	0.39	5.2	7.6	2239	84.5	20.7	99.9	197.2	5.9	3
22	2018/07/15 20:42	2018/07/16 12:57	16.3	10.70	1346	0.40	4.9	7.1	2522	84.6	20.4	99.9	193.5	4.3	2
23	2018/07/16 20:43	2018/07/17 17:35	20.9	15.28	1147	0.33	4.9	6.8	2078	84.5	19.5	100.0	196.1	4.9	2
24	2018/07/17 22:07	2018/07/18 11:47	13.7	8.44	1250	0.41	4.9	7.5	2534	84.5	20.0	100.0	199.0	6.4	1
25	2018/07/18 21:36	2018/07/19 11:06	13.5	10.37	1161	0.31	4.6	6.9	2070	84.6	19.4	99.9	200.8	6.8	1
26	2018/07/19 22:51	2018/07/20 12:59	14.1	9.16	1157	0.41	5.2	7.5	2382	84.5	19.7	100.0	192.9	5.2	2
27	2018/07/20 22:27	2018/07/21 03:02	4.6	12.48	938	0.15	3.8	6.0	1237	84.5	18.7	99.8	210.9	6.4	1
28	2018/07/21 23:03	2018/07/21 23:36	0.6	21.02	607	0.06	3.2	5.5	622	84.6	18.4	98.9	199.4	7.1	0
29	2018/07/22 22:49	2018/07/22 23:34	0.8	7.22	1437	0.19	3.5	5.7	1658	84.4	18.6	99.2	81.3	9.7	0
30	2018/07/23 03:46	2018/07/23 18:29	14.7	1.87	630	0.37	6.0	9.8	1859	83.9	18.4	99.9	64.4	13.7	2
31	2018/07/24 09:03	2018/07/24 10:09	1.1	2.30	148	0.07	5.7	7.9	381	84.1	18.8	100.0	272.0	8.3	0
32	2018/07/24 11:34	2018/07/24 12:03	0.5	5.42	130	0.03	4.3	7.1	244	84.1	19.5	100.0	257.6	5.9	0
33	2018/07/24 18:20	2018/07/25 08:52	14.5	8.18	1441	0.23	3.7	6.1	1846	84.1	20.2	99.9	220.1	11.9	1
34	2018/07/25 19:29	2018/07/25 20:44	1.3	21.54	166	0.01	2.7	5.0	220	84.3	21.6	99.0	223.7	9.0	0
35	2018/07/26 01:38	2018/07/26 05:25	3.8	9.86	770	0.11	3.6	6.0	939	84.4	20.7	99.8	219.0	3.6	0
36	2018/07/26 19:32	2018/07/27 01:04	5.5	23.67	326	0.06	3.8	5.5	775	84.5	19.3	98.4	149.4	6.6	0
37	2018/07/27 12:17	2018/07/27 14:44	2.4	24.69	455	0.13	4.7	6.1	1185	84.5	20.0	94.5	89.9	4.5	0
38	2018/07/27 16:45	2018/07/30 00:05	55.3	10.68	445	0.17	5.1	7.3	1187	84.4	18.7	99.1	160.8	4.3	5
39	2018/07/30 03:55	2018/07/30 04:25	0.5	10.83	279	0.09	4.9	7.4	563	84.3	18.5	99.1	268.2	1.1	0
40	2018/07/30 06:29	2018/07/30 12:41	6.2	27.45	209	0.06	4.8	6.4	477	84.4	20.3	95.2	83.9	2.7	0

Table S2. Estimated updraft velocity (v_{up}) (means ± S.D.), estimated cloud base height (*CBH*) (means ± S.D.) and the sensitivities analysis of N_C to N_P, *CBH* and v_{up} during CP-1 and CP-2.

	v_{up} m s^{-1}	*CBH* m	[a,b]$\partial \ln N_C / \partial \ln N_P (R^2)$	[b]$\partial \ln N_C / \partial \ln CBH (R^2)$	[b]$\partial \ln N_C / \partial \ln v_{up} (R^2)$
CP-1	0.82 ± 0.29	1017.9 ± 301.5	0.544(0.2820)	-0.118(0.0018)	0.275(0.0599)
CP-2	0.92 ± 0.36	1040.4 ± 260.2	0.144(0.0500)	0.216(0.1279)	0.868(0.1167)

[a]The value of $\partial \ln N_C / \partial \ln N_P$ was equal to AIE_N

[b]R^2 represented correlation coefficient

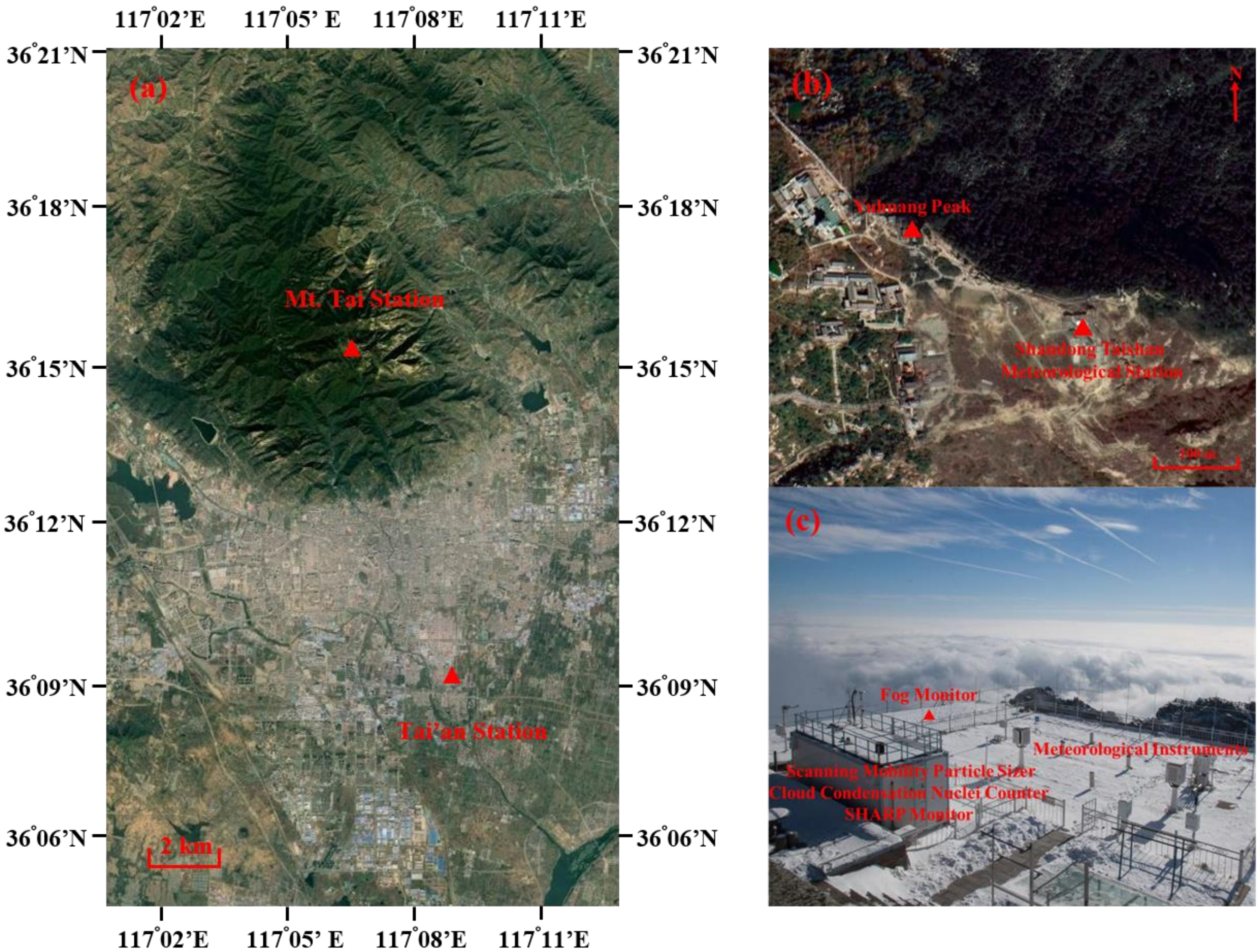

Figure S1. The pictures and schematic of (a) the geographic position of Mt. Tai and Tai'an (©Google Maps) (b) the observation station at Mt. Tai (©Google Maps) (c) the arrangement of instruments in Shandong Taishan Meteorological Station (http://p.weather.com.cn/2016/12/2638460.shtml). The corresponding sampling tubes were at least 1.5 m higher than the roof and at least 1.0 m away from each other to avoid the mutual interference.

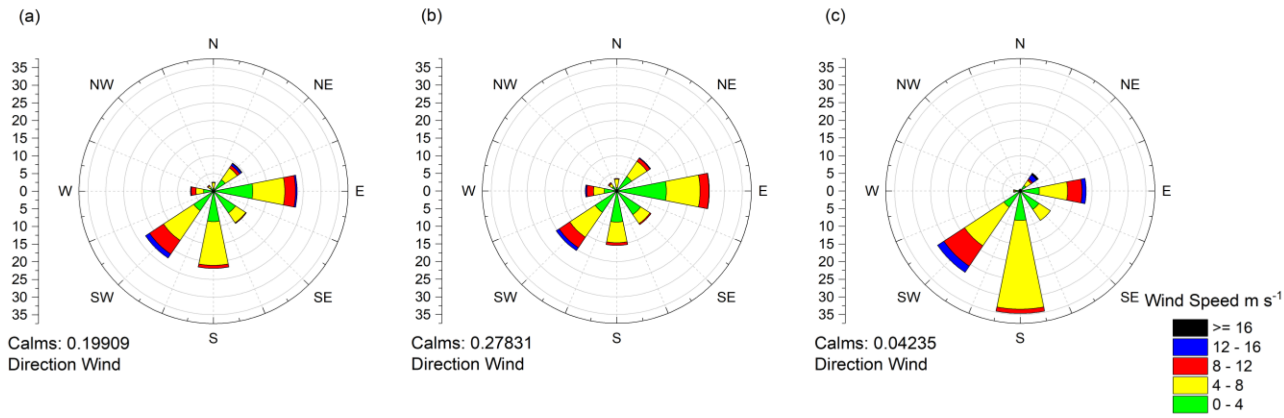

Figure S2. Wind direction and wind speed a) during the whole summer campaign at Mt. Tai, b) without cloud events and c) during cloud events.

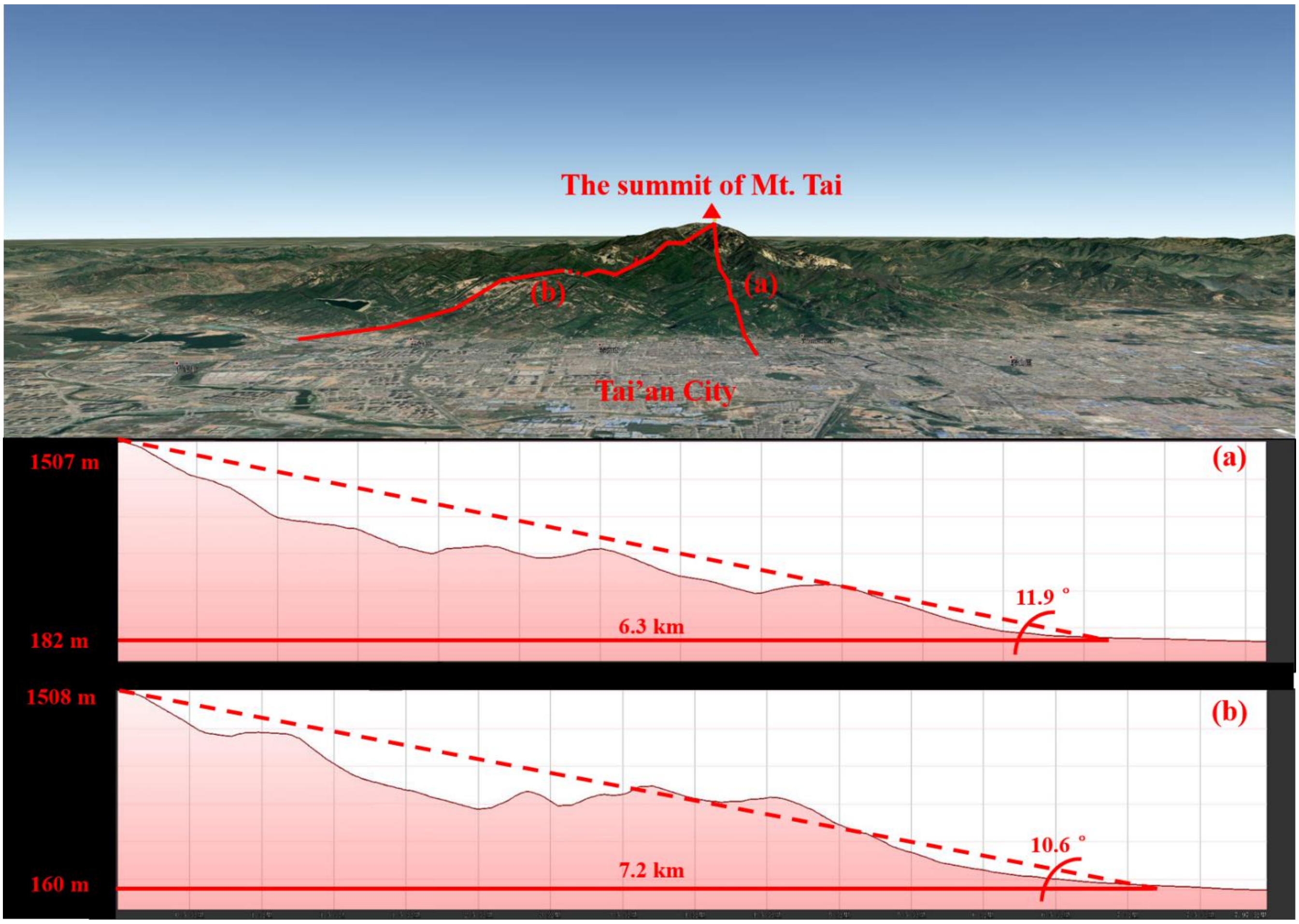

Figure S3. Influence of the topography on the vertical wind field at monitoring station. The topographic images at Mt. Tai were originated from ©Google Earth. Taking (a) the south-north transect of Mt. Tai for CP-1 and (b) the southwest-northeast transect of Mt. Tai for CP-2 to estimate the inclination angles and updraft velocities.

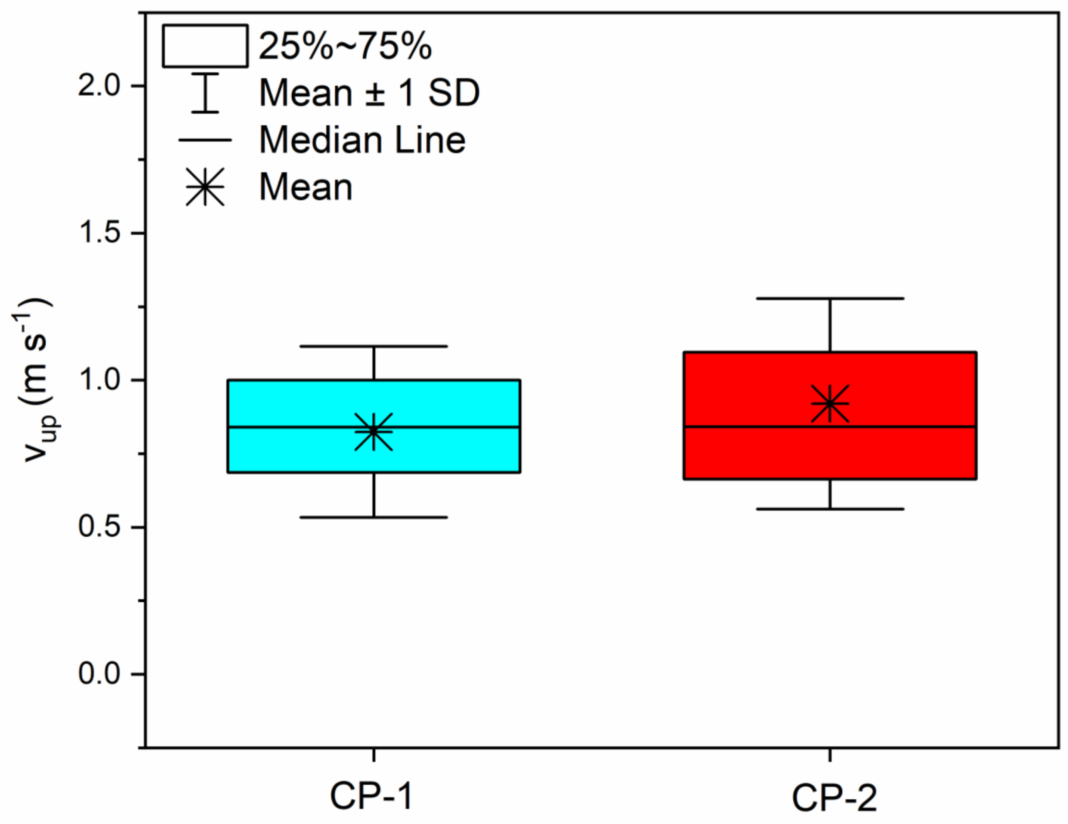

Figure S4. The box plot of calculated v_{up} (m s^{-1}) during CP-1 (blue) and CP-2 (red).

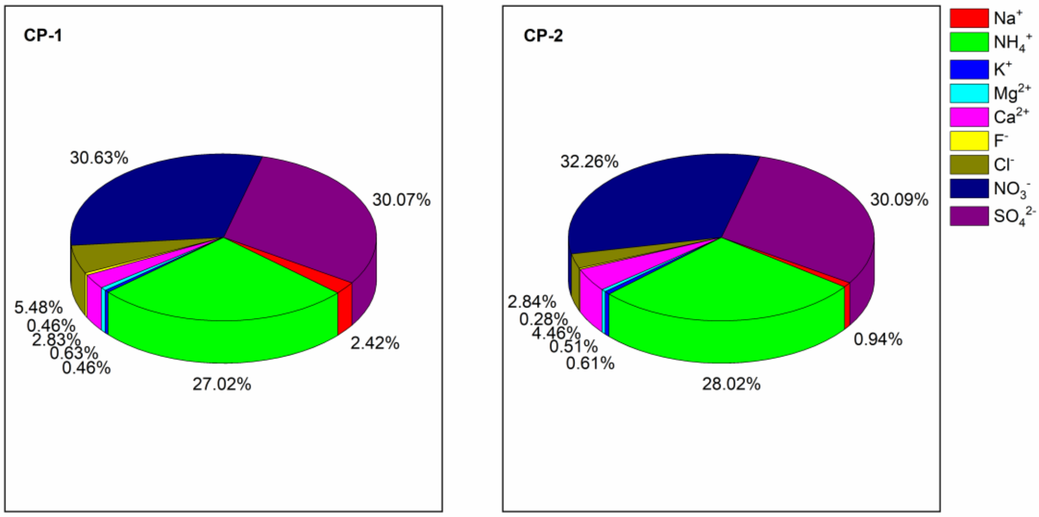

Figure S5. The averaged inorganic chemical compositions of cloud samples collected during CP-1 and CP-2. Each cloud process contained 12 cloud samples.

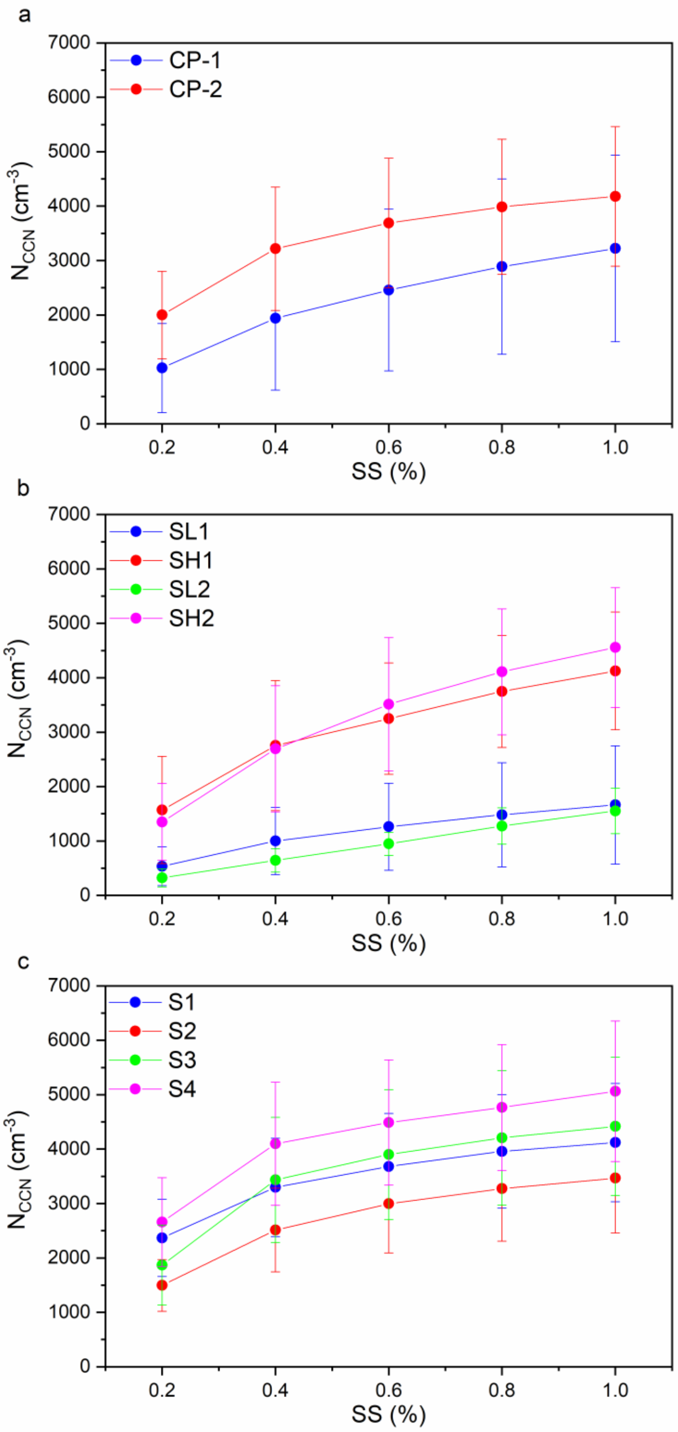

1

2 **Figure S6: The N_{CCN} measured at *SS* = 0.2%, 0.4%, 0.6%, 0.8% and 1.0% during (a) CP-1 and CP-2 (b) SL1, SH1, SL2**

3 **and SH2 (c) S1, S2, S3 and S4.**

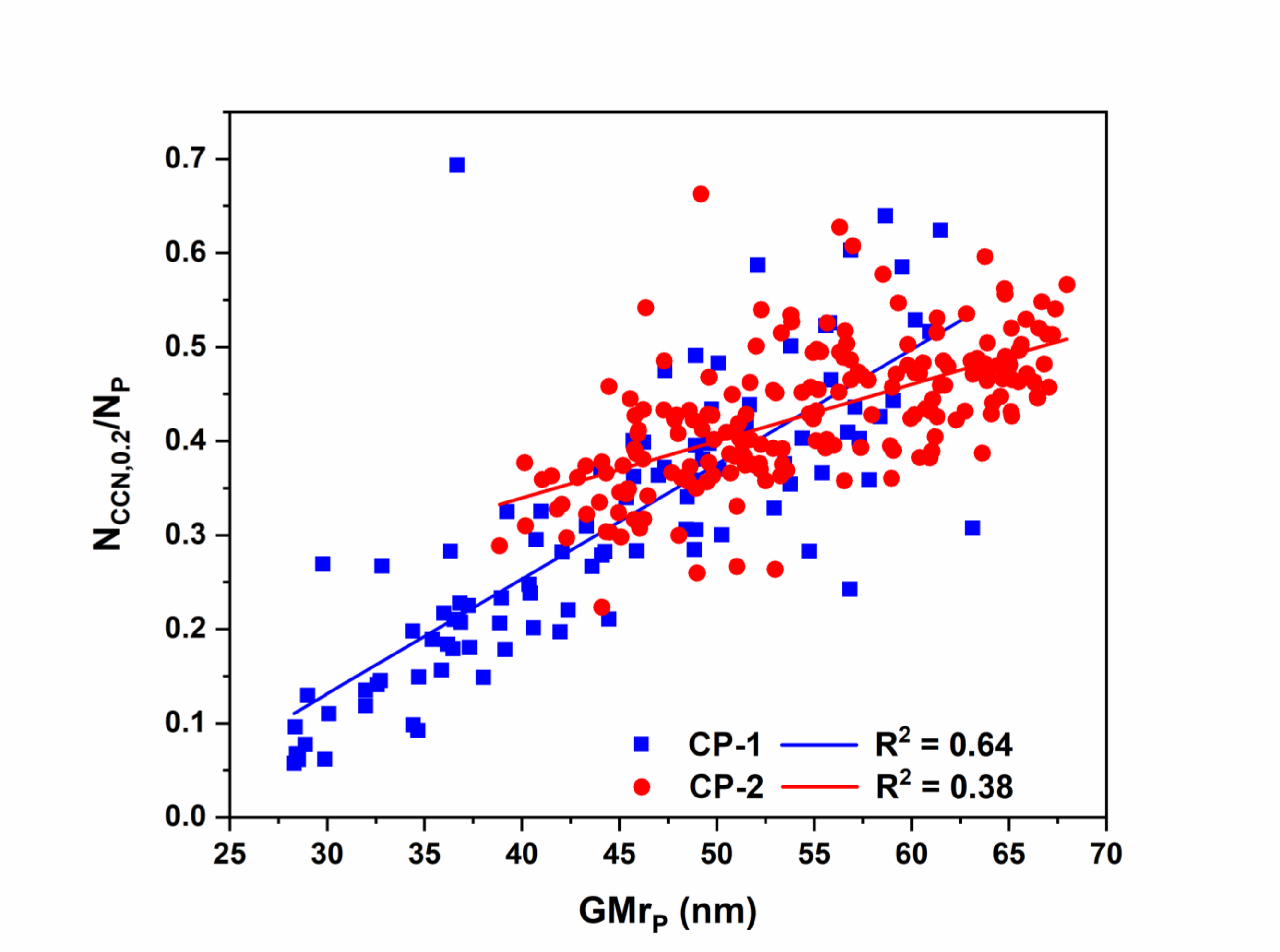

Figure S7. The scatter plot of $N_{CCN,0.2}/N_p$ with GMr_P (geometric mean radius of aerosol particles) during CP-1 (blue) and CP-2 (red). The lines represent the linear fitting of data points.

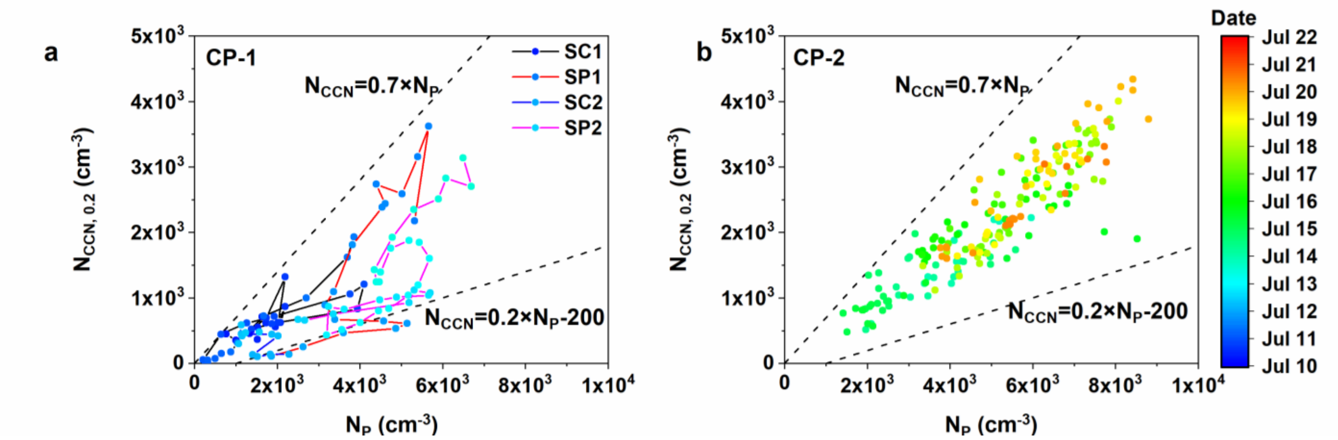

Figure S8. The plot of $N_{CCN,0.2}$ versus N_P (a) in CP-1 (b) in CP-2. The two dashed lines are the visually defined boundaries from the study of Asmi et al. (2012).

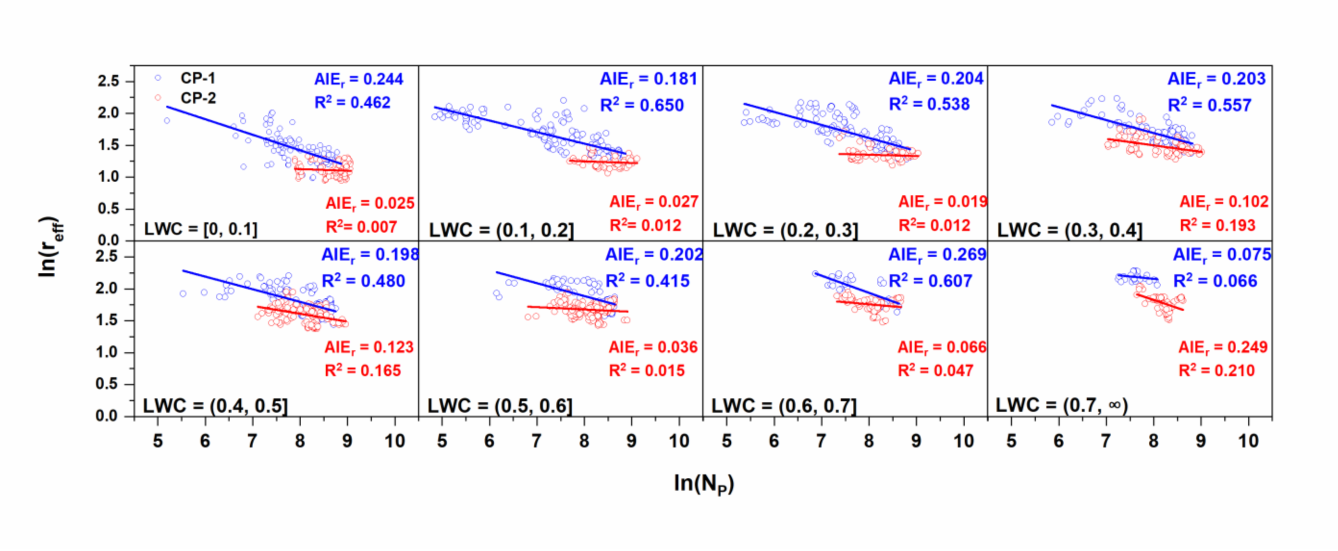

Figure S9: The calculation of AIE_r based on the plot of r_{eff} versus N_P in narrow LWC size bins with increase of 0.1 g m^{-3}.

Reference

Asmi, E., Freney, E., Hervo, M., Picard, D., Rose, C., Colomb, A., and Sellegri, K.: Aerosol cloud activation in summer and winter at puy-de-Dome high altitude site in France, Atmos. Chem. Phys., 12, 11589-11607, 10.5194/acp-12-11589-2012, 2012.

Hammer, E., Bukowiecki, N., Gysel, M., Juranyi, Z., Hoyle, C. R., Vogt, R., Baltensperger, U., and Weingartner, E.: Investigation of the effective peak supersaturation for liquid-phase clouds at the high-alpine site Jungfraujoch, Switzerland (3580 m a.s.l.), Atmospheric Chemistry and Physics, 14, 1123-1139, 10.5194/acp-14-1123-2014, 2014.

Spiegel, J. K., Zieger, P., Bukowiecki, N., Hammer, E., Weingartner, E., and Eugster, W.: Evaluating the capabilities and uncertainties of droplet measurements for the fog droplet spectrometer (FM-100), Atmospheric Measurement Techniques, 5, 2237-2260, 10.5194/amt-5-2237-2012, 2012.

Verheggen, B., Cozic, J., Weingartner, E., Bower, K., Mertes, S., Connolly, P., Gallagher, M., Flynn, M., Choularton, T., and Baltensperger, U.: Aerosol partitioning between the interstitial and the condensed phase in mixed-phase clouds, Journal of Geophysical Research-Atmospheres, 112, 13, 10.1029/2007jd008714, 2007.